short-term experiments because of the rapid disappearance of the human NK cells (3). Although the latter is more suitable for long-term observation, the number of human NK cells was not always sufficient (4, 6), and exogenous administration of human IL-15 was needed to increase the population (5, 7).

In the course of modifying the NOD/Shi-*scid*-IL-2Rγ^{null} (NOG) mouse to produce the next generation of humanized mice (8–10), we established a NOG mouse substrain expressing human IL-2 (NOG–IL-2 Tg). In this study, we used this novel mouse strain as a recipient for HSCs; this resulted in unexpected differentiation of predominantly human NK cells in these mice. These human NK cells were killer cell Ig-like receptor (KIR)-expressing mature cells and showed the IL-2–activated phenotype. In addition, they strongly inhibited in vivo tumor formation. The NOG–IL-2 Tg will become a suitable platform for studying human NK cells in vivo.

Materials and Methods

Mice

NOG and NOD/ShiJic IL-2Rγ^{null} mice were used in this study. Both strains were maintained in the Central Institute for Experimental Animals under specific pathogen–free conditions.

To generate the human IL-2–expressing transgenic NOG mouse, a DNA fragment containing human IL-2 cDNA, under the control of the CMV promoter, was microinjected into fertilized eggs of NOD/ShiJic IL-2Rγ^{null} mice. Founder mice were backcrossed with NOG mice to obtain NOG–IL-2 Tg mice (formally, NOD.Cg-*Prkdc*^{scid}*il2rg*^{tm1Sug} *Tg (CMV-IL2)4-2Jic*/Jic).

All experiments were performed in accordance with institutional guidelines (11004, 14038R), which were approved by the Animal Experimentation Committee of the Central Institute for Experimental Animals.

Measurement of IL-2

To quantify human IL-2 in NOG–IL-2 Tg mice, PB was collected from the orbital venous plexus of 5-wk-old mice using heparin (Novo-heparin; Mochida Pharmaceutical, Tokyo, Japan)-coated capillaries (Drummond Scientific, Broomall, PA) under anesthesia. IL-2 concentration in the plasma was determined by ELISA (BD Biosciences, San Jose, CA). The average was 1–3 ng/ml, and none was detected in the plasma of non-transgenic (non-Tg) mice (Fig. 1A). To measure IL-2 produced by various tissues of NOG–IL-2 Tg mice, the mice were perfused with PBS under anesthesia. The spleen, liver, lung, kidney, and heart were isolated and cut into small pieces with a razor blade and incubated for 1 h at 37°C in RPMI 1640. After incubation, IL-2 concentration in the supernatants was quantified by ELISA. The total amount of IL-2 during the incubation was calculated by multiplying the concentration of IL-2 by the volume of RPMI 1640.

Transplantation of human HSCs

We used umbilical cord blood (CB)-derived CD34$^+$ progenitor/stem cells from white humans (Lonza, Basel, Switzerland) and Japanese CB-derived CD34$^+$ stem cells (RIKEN BRC, Tsukuba, Japan). For xeno-transplantation, 8-wk-old adult mice were subjected to x-irradiation (2.5 Gy) (MBR-1505R; Hitachi Medical, Tokyo, Japan), and 2–5 $\times$ 10^4 HSCs were transplanted i.v. within 24 h. To monitor human hematopoiesis, the mice were bled every other week for 3 mo, and the mononuclear cells (MNCs) were analyzed by flow cytometry.

Preparation of immune cells in tissues of HSC-transferred mice

HSC-transferred mice were euthanized to collect PB from an abdominal vein under anesthesia. Blood plasma was separated by centrifugation. Bone marrow (BM) cells were obtained by flushing femurs with 1 ml PBS containing 2% FBS. Spleen cells and lymphocytes in the liver were prepared by smashing the tissues between two glass slides, and the tissue debris was removed by nylon mesh. Lungs were treated with 1 mg/ml collagenase and 50 ng/ml DNase in RPMI 1640 (Life Technologies, Grand Island, NY) for 30 min at 37°C, followed by filtration through mesh. Mouse RBCs were eliminated with RBC lysing solution (Pharm Lyse; BD Biosciences). After washing, the cell pellet was resuspended with PBS + 2% FBS.

Purification of human NK cells

Human PB was obtained from healthy volunteers after acquiring their informed consent. MNCs (human PBMCs [hPBMCs]) from normal human PB were prepared by density centrifugation on Ficoll (Lymphoprep; Axis-Shield, Oslo, Norway). Human CD56$^+$ NK cells were negatively selected from hPBMCs or splenocytes of HSC-transferred mice between 4 and 6 wk post-HSC transplantation. Using a human NK cell isolation kit (Miltenyi Biotec, Bergisch Gladbach, Germany) in combination with biotin-conjugated anti-mouse CD45 mAb (BD Biosciences), all cells, with the exception of human CD56$^+$ NK cells, were magnetically labeled and eliminated using a MACS LD column (Miltenyi Biotec). The purity of the isolated human NK cells was usually >90%.

In some experiments, we used commercially available white human NK cells (AllCells, San Diego, CA).

Flow cytometry

The single MNC suspensions were stained with appropriate Abs for 30 min at 4°C in the dark. After washing with FACS buffer (PBS, 1% FBS, 0.1% NaN_3), the cells were resuspended in FACS buffer containing propidium iodide. We used a FACSCanto (BD Biosciences) for multicolor flow cytometric analysis; the data were analyzed using FACSDiva software (ver. 6.1.3; BD Biosciences).

The following Abs were used. Anti-human CD16-FITC and anti-human CD3-FITC were purchased from eBioscience (San Diego, CA). Alexa Fluor 488–conjugated anti-human NK group 2 membrane C (NKG2C) was from R&D Systems (Minneapolis, MN). Anti-human CD33-FITC, anti-human CD3-PE, anti-human CD69, anti-mouse CD45-allophycocyanin, and anti-human CD45–allophycocyanin–Cy7 were from BD Biosciences. Anti-human CD34-FITC, anti-human CD56-PE, anti-human CD159a (NKG2A)-PE, and anti-human NKp80-PE were from Beckman Coulter (Miami, FL). All of the following Abs against human Ags were from BioLegend (San Diego, CA): FITC-conjugated anti-CD158a/h and anti-CD158e1; PE-conjugated anti-CD56, anti-NKp30, anti-NKp44, anti-NKp46, anti-CD57, anti-CD107a, anti-CD127, anti-NKG2D, anti-CD158b, and anti-CD158f; PE-Cy7–conjugated anti-CD3, anti-CD19, anti-CCR4, and anti-CD117; and allophycocyanin-conjugated anti-CD16, anti-CD94, and anti–HLA-DR.

The absolute number of cells was calculated using fluorescent beads (Flow-Count; Beckman Coulter), according to the manufacturer's instructions.

Cell culture

Purified human NK cells were cultured in complete RPMI 1640 medium (Life Technologies, Carlsbad, CA), supplemented with 10% FBS, 2 nM MEM nonessential amino acids, 50 nM 2-ME, 100 U/ml penicillin, and 100 μg/ml streptomycin. In some experiments, the cells were stimulated with 2 nM IL-2, 2 ng/ml IL-12, or 2 ng/ml IL-15 (Miltenyi Biotec), either alone or in various combinations. The cells also were stimulated with 50 ng/ml PMA and 1 μg/ml ionomycin. K562 (human erythromyeloblastoid leukemia cell line) and L428 (human CCR4$^+$ Hodgkin's lymphoma cell line; a kind gift from Dr. Takashi Ishida, Department of Medical Oncology and Immunology, Nagoya City University, Japan) were cultured in complete RPMI 1640 medium. HeLaS3 (human cervical cancer cell line) was cultured in Ham/F12 medium supplemented with 10% FBS, 2 nM nonessential amino acids, 50 nM 2-ME, and antibiotics.

Typing of KIR mRNA

Expression patterns of mRNA encoding inhibitory KIRs in human NK cells were examined using a KIR typing kit (Miltenyi Biotec), according to the manufacturer's instructions. Briefly, total RNA was purified from human NK cells using NucleoSpin TriPrep (MACHEREY-NAGEL, Dueren, Germany). First-strand cDNA was synthesized from the total RNA using the SuperScript III reverse transcriptase system (Invitrogen, Carlsbad, CA) and subjected to KIR typing.

Cytotoxicity assay

Cytotoxic activity of human NK cells was measured using K562 and HeLaS3 as target cells. The target cells were labeled with ^{51}Cr and then cultured with human NK cells for 4 h at 37°C. The amount of ^{51}Cr released into the culture supernatant was measured with a gamma counter (ARC-300; Hitachi-Aloka Medical, Tokyo, Japan). In some experiments, human NK cells were cultured in the presence of various human cytokines for 2 d and then incubated with K562 tumor cells for 4 h. The E:T ratio was 10:1. The release of lactate dehydrogenase into the culture supernatant was

measured using a CytoTox96 Non-Radioactive Cytotoxicity Assay kit (Promega, Fitchburg, WI).

Intracellular staining

To investigate the expression of perforin, granzyme A, and IFN-γ in human NK cells, purified human NK cells were stimulated for 20 h at 37°C in the presence of 3 μg/ml brefeldin A. After the cells were stained with Abs for surface Ags, they were fixed in paraformaldehyde and subsequently permeabilized using Perm/Fix solution (BD Biosciences). The permeabilized cells were stained with anti-human granzyme A–FITC, anti-human perforin-PE, or anti-human IFN-γ–PE (BioLegend) in Perm/Fix solution for 30 min at room temperature. After washing, the cells were resuspended with FACS buffer and analyzed by FACSCanto.

To detect the phosphorylation of STAT5, PB-derived NK (PB-NK) or splenic NK cells from human cord-blood–derived HSC (hu-HSC) NOG–IL-2 Tg mice were cultured at 37°C in the presence or absence of rIL-2 for the indicated periods and subsequently fixed with Fixation Buffer (BD Biosciences). After washing with FACS buffer three times, the cells were resuspended with Perm Buffer III (BD Biosciences) and incubated for 30 min on ice. After washing four times, the cells were stained with Alexa Fluor 488–labeled anti-STAT5 (pY694) or Alexa Fluor 488–labeled mouse IgG1 as an isotype control (BD Biosciences) for 60 min at 37°C. The cells were analyzed by FACSCanto after washing.

Quantification of perforin by ELISA

Perforin levels in blood plasma from HSC-reconstituted NOG mice were measured using a perforin-specific ELISA kit (Abcam, Cambridge, U.K.).

Quantification of mRNA

First-strand cDNA was synthesized from 10 ng total RNA from human CD56$^+$ NK cells using SuperScript III reverse transcriptase. Subsequently, the cDNA was subjected to quantitative real-time PCR (qPCR) analysis using SYBR premix ExTaq II and Thermal Cycler Dice (both from Takara Bio, Shiga, Japan). Human GAPDH primers were purchased from Takara Bio (HA067812-F and HA067812-R). The primers for human granzyme A (GZMA: PPH00314E) and perforin (PRF1: PPH07126A) were from QIAGEN (Valencia, CA). The comparative Ct method was used for data analysis.

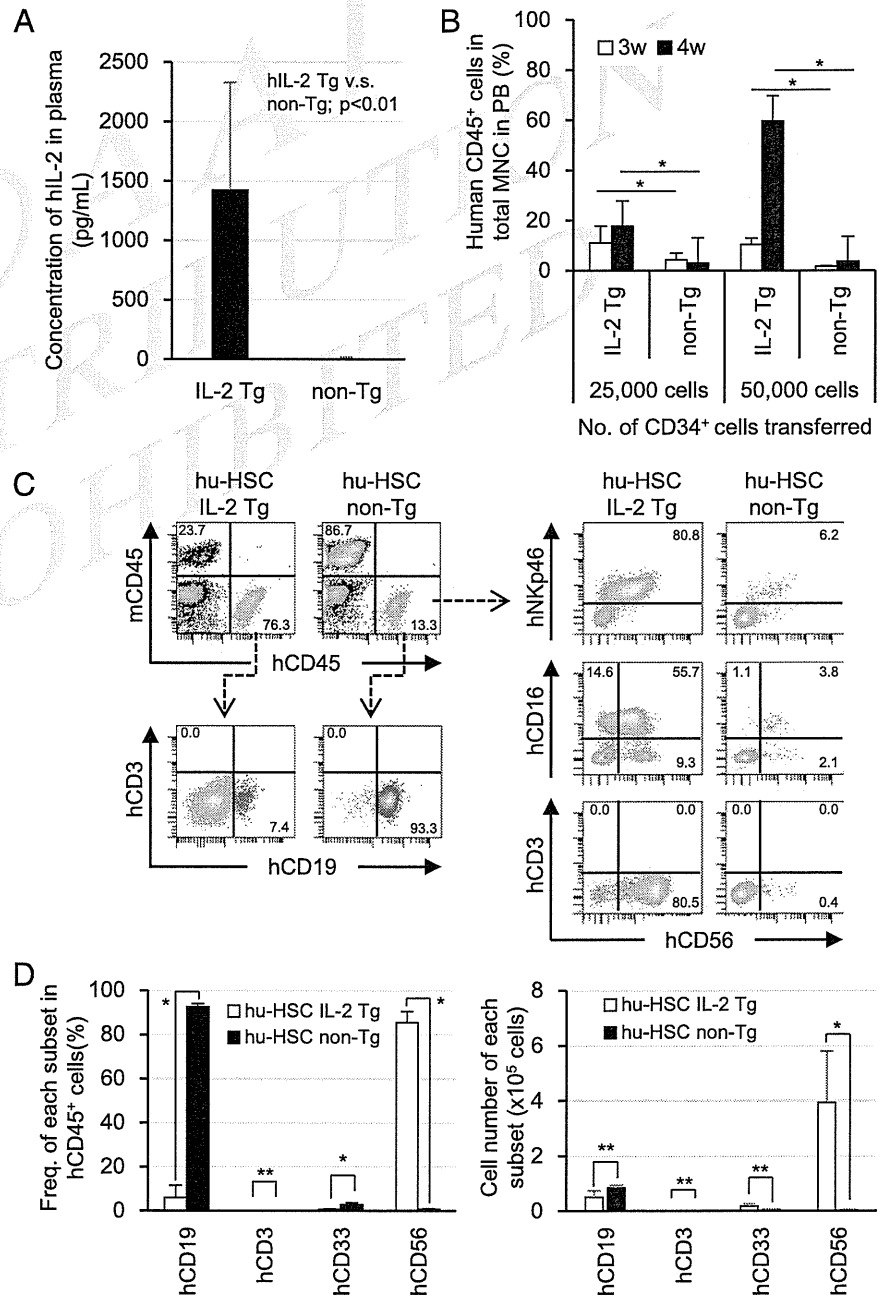

FIGURE 1. Development of human NK cells in human HSC-transferred NOG–IL-2 Tg mice. (**A**) The concentration of human IL-2 in plasma of NOG–IL-2 Tg Tg mice (n = 53) or non-Tg NOG mice (n = 18). (**B**) High engraftment of human CD45$^+$ cells in hu-HSC NOG–IL-2 Tg mice. NOG–IL-2 Tg (n = 26) or non-Tg NOG mice (n = 16) were reconstituted with 2.5 × 10^4 or 5 × 10^4 CD34$^+$ HSCs and analyzed 3 and 4 wk after transplantation. The frequencies (mean ± SD) of human CD45$^+$ cells among MNCs in PB are shown. (**C**) Development of CD3$^-$ CD56$^+$NKp46$^+$ human NK cells in hu-HSC NOG–IL-2 Tg mice. Representative FACS plots of the PB of humanized mice 6 wk post-HSC transplantation. Human CD45$^+$ cells were gated (represented by red dots) and analyzed further for surface Ags. Human B cells are represented by blue dots, and NKp46$^+$ human NK cells are represented by green dots. Data of three independent experiments using a total of four mice/group are shown. (**D**) Predominant development of human NK cells in hu-HSC NOG–IL-2 Tg mice. The frequencies and absolute numbers (mean ± SD) of various subpopulations obtained from (C) are shown. Student t test was used to identify significant differences.

In vivo tumor transplantation model

To examine the in vivo killing activity of human NK cells developed in HSC-reconstituted NOG–IL-2 Tg mice, K562 (2.5×10^5 in 0.1 ml of PBS) was inoculated s.c. into the midline of the dorsal region of the mice.

To examine the in vivo ADCC activity, L428 (5×10^6 in 0.1 ml of PBS) was inoculated s.c. into HSC-reconstituted NOG–IL-2 Tg mice. From 2 wk posttumor inoculation, when the tumor became visible, defucosylated anti-human CCR4 mAb (100 μg in 0.2 ml saline), mogamulizumab (Poteligeo; Kyowa-Kirin, Tokyo, Japan) was administered i.p. twice each week for 4 wk.

Solid tumor size was measured weekly using micrometer calipers and calculated using the following formula: tumor volume (mm^3) = 1/2 × length (mm) × [width (mm)]^2.

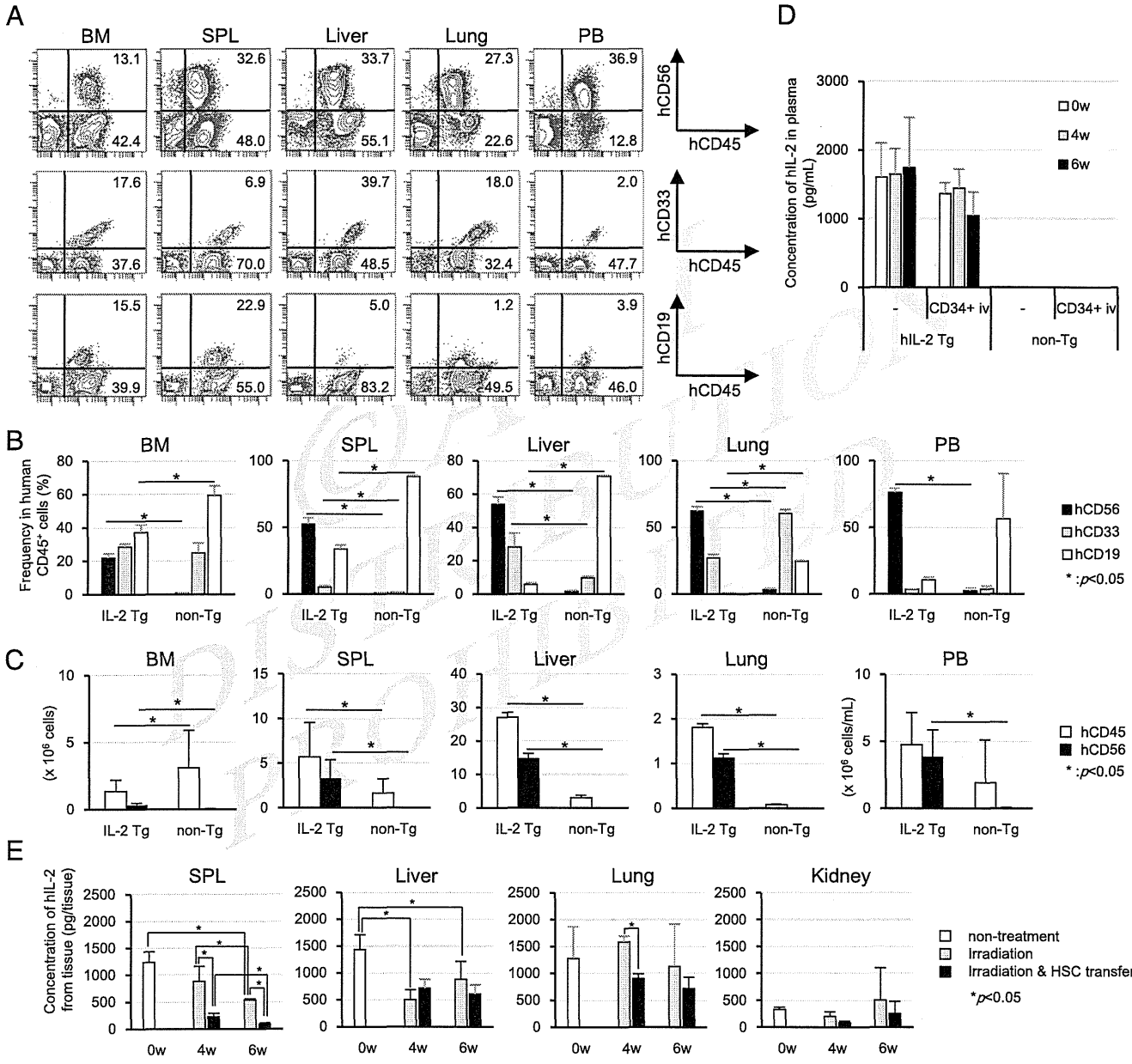

FIGURE 2. Distribution of human CD56$^+$ NK cells among various tissues in human HSC-transferred NOG–IL-2 Tg mice. (**A**) Distribution of human CD56$^+$ NK cells among various tissues. BM, spleen, PB, liver, and lung of hu-HSC NOG–IL-2 Tg mice were analyzed at 6 wk after HSC transfer. Single-cell suspensions were prepared from each organ of NOG–IL-2 Tg mice and stained with anti-human CD45, CD56, CD33, and CD19 Abs. Representative data from three independent experiments are shown. Frequencies of CD56$^+$ NK cells, CD33$^+$ myeloid cells, or CD19$^+$ B cells (**B**) and absolute numbers of human CD45$^+$ and CD45$^+$CD56$^+$ NK cells in tissues of humanized mice (**C**). Cells were counted after preparation of single-cell suspensions, as described in (A). The absolute numbers of human CD45$^+$ and CD45$^+$CD56$^+$ NK cells were calculated by multiplying the subset frequencies by the total cell numbers. The averages ± SD from a total of six mice for each group are shown. A total of three mice/group was used for analysis of the liver and lung. (**D**) The concentration of human IL-2 in plasma of hu-HSC NOG–IL-2 Tg mice. Plasma was collected from hu-HSC NOG–IL-2 Tg or hu-HSC non-Tg NOG mice at 0, 4, or 6 wk after HSC transplantation. The level of human IL-2 was determined by ELISA ($n = 9$ for 0 wk, $n = 6$ for 4 wk, and $n = 3$ for 6 wk). (**E**) IL-2 production in tissues of hu-HSC NOG–IL-2 Tg mice. Each tissue was isolated from mice after perfusion with PBS, as described in *Materials and Methods*, and incubated in RPMI 1640. The supernatants were recovered after 1 h, and the concentration of human IL-2 was measured by ELISA. The total amount of IL-2 was obtained by multiplying the concentration by the volume of RPMI 1640. Representative data from three independent experiments are shown. The Student t test was used to identify significant differences.

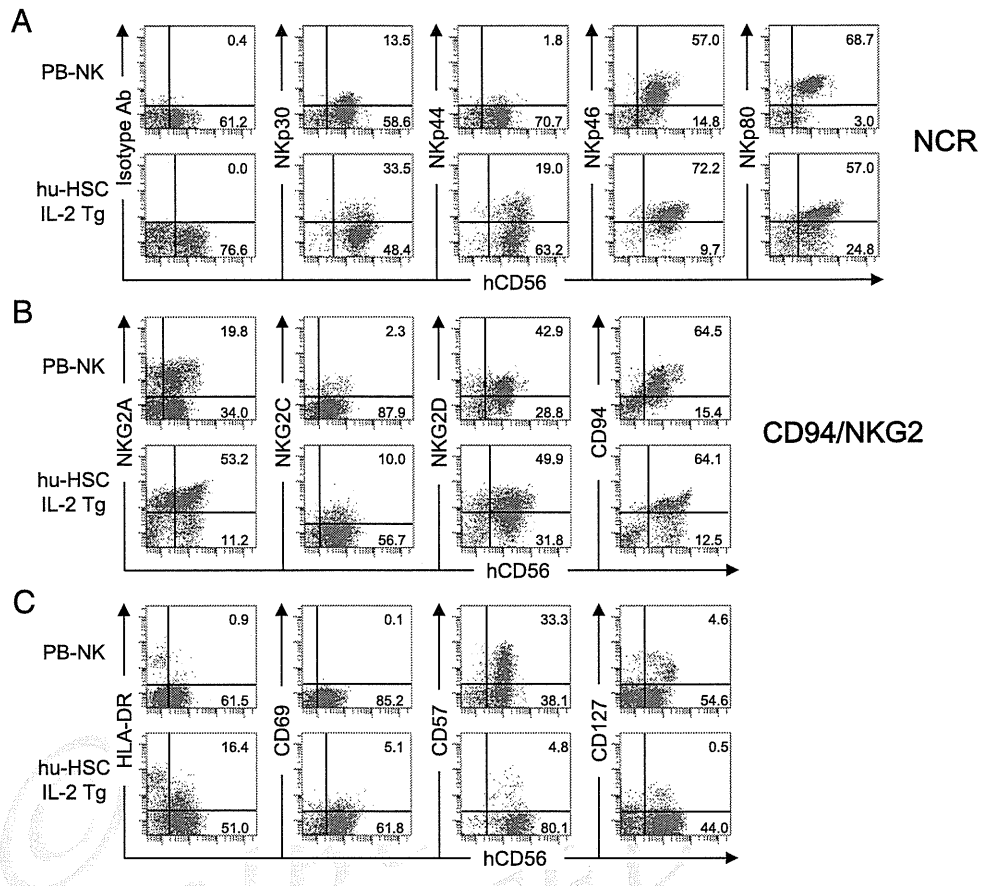

FIGURE 3. Expression of NK cell receptors in human NK cells in hu-HSC NOG–IL-2 Tg mice. Representative FACS plots of human NK receptors are shown. Splenocytes of hu-HSC NOG–IL-2 Tg mice 6 wk after HSC transplantation and normal human CD56$^+$ PB-NK cells, which were negatively selected by MACS, were analyzed by FACS after staining with Abs for NCR (**A**), NKG2 family receptors and CD94 (**B**), and various Ags, including activation markers (**C**). Representative data from three independent experiments are shown.

Results

After transfer of human HSCs into NOG–IL-2 Tg mice (hu-HSC NOG–IL-2 Tg), human hematopoietic cells differentiated more efficiently than in conventional non-Tg NOG mice (Fig. 1B). F1 Within 4 wk posttransfer of HSC, human CD45$^+$ cells had expanded considerably in the PB of NOG–IL-2 Tg mice compared with non-Tg NOG mice (Fig. 1B). Flow cytometric analysis demonstrated that NKp46$^+$CD56$^+$CD3$^-$ cells had differentiated predominantly in the NOG–IL-2 Tg mice, suggesting that they were NK cells, whereas mostly CD19$^+$ B cells were seen in the non-Tg mice. These CD56$^+$CD3$^-$ cells consisted of CD16$^+$ and CD16$^-$ cells (Fig. 1C). The predominance of NK cells in hu-HSC NOG–IL-2 Tg among human CD45$^+$ cells in the PB also was confirmed at 6 wk post-HSC transplantation (Fig. 1D). Analysis of various organs indicated that CD56$^+$ cells were present in the BM of hu-HSC NOG–IL-2 Tg mice, and their abundance was confirmed in all of the tissues examined (Fig. 2A, 2B). F2 Most of the human CD45$^+$CD56$^-$ cells in the spleen were CD19$^+$ B cells, and CD33$^+$ human myeloid cells in the liver and lung (Fig. 2A). Q:16 The absolute number of CD56$^+$ human NK cells in hu-HSC NOG–IL-2 Tg mice was >10-fold higher than in hu-HSC non-Tg NOG mice (Fig. 2C). To examine the influence of the development of human NK cells on the level of IL-2 in NOG–IL-2 Tg mice, we quantified the amount of IL-2 in plasma at various time points. HSC transplantation into NOG–IL-2 Tg mice induced no significant change (Fig. 2D). To investigate the production of IL-2 in various tissues, we isolated spleen, liver, lung, heart, and kidney after perfusion with PBS to exclude the contamination by blood. Because the homogenized tissue lysates produced high background signals, irrespective of the IL-2 transgene, we instead cut the tissues into small pieces, incubated them for 1 h at 37°C in RPMI 1640, and quantified the released IL-2. The spleen, liver, lung, and kidney produced a significant amount of IL-2 (Fig. 2E), whereas a low amount was detected in the heart (data not shown). Interestingly, the production of IL-2 in the spleen and liver, but not in the lung and kidney, in NOG–IL-2 Tg mice was reduced significantly by x-irradiation alone (Fig. 2E). The development of human NK cells in NOG–IL-2 Tg mice also influenced the IL-2 level (Fig. 2E). Indeed, the spleen or lung of hu-HSC NOG–IL-2 Tg mice produced lower amounts of IL-2 at 4 and 6 wk or 4 wk after HSC trans-

Table I. ΔMFI for human NK surface markers from PB-NK cells and hu-HSC NOG–IL-2 Tg mice

	NCR				NKG2 Family			
	NKp30	NKp44	NKp46	NKp80	NKG2A	NKG2C	NKG2D	CD94
PB-NK	124 ± 9	15 ± 6	551 ± 196	1214 ± 153	529 ± 61	669 ± 508	412 ± 151	612 ± 185
hu-HSC-IL-2 Tg	470 ± 190	318 ± 152	1044 ± 263	658 ± 198	1962 ± 245	400 ± 44	809 ± 384	1196 ± 235
p value	0.0032	0.0030	0.0026	0.021	1.2E−6	0.23	0.044	0.0058

ΔMFI = MFI (Ab) − MFI (isotype control) in CD56$^+$ cells.
MFI, mean fluorescence intensity.

plantation, respectively, compared with nontransplanted NOG–IL-2 Tg mice. In contrast, the liver and kidney did not show such a reduction. It should be noted that there is a possibility that human NK cells residing in those tissues consumed IL-2 during the incubation.

To explore the characteristics of the CD56$^+$ cells in hu-HSC NOG–IL-2 Tg mice, we examined the expression levels of various NK cell receptors. With regard to natural cytotoxicity receptor (NCR), human NK cells from hu-HSC NOG–IL-2 Tg mice expressed higher levels of NKp30, NKp44, and NKp46 than did normal PB-NK cells, whereas the level of NKp80 was lower than that in normal PB-NK cells (Fig. 3A, Table I). With regard to the NKG2 family, the activating receptor NKG2C, a C-type lectin-like receptor specific for HLA-E, was detected in a subset of NK cells of hu-HSC NOG–IL-2 Tg mice (Fig. 3B, Table I). The expression of NKG2D, another C-type lectin-like receptor specific for stress-inducing molecules was higher in NK cells from hu-HSC NOG-IL-2 Tg mice than that in normal PB-NK cells (Fig. 3B, Table I). The frequency of NK cells expressing NKG2A, a receptor that transmits inhibitory signals, was increased in hu-HSC NOG–IL-2 Tg mice compared with normal PB-NK cells, and the amount of the molecule also was higher in the former (Fig. 3B, Table I). The expression of CD94, which forms heterodimers with various NKG2 molecules to transmit both activating and inhibitory signals, was also higher in NK cells from hu-HSC NOG–IL-2 Tg mice than in PB-NK cells (Fig. 3B, Table I). Furthermore, some human NK cells of hu-HSC NOG–IL-2 Tg mice expressed a significant amount of HLA-DR or CD69 activation markers (Fig. 3C). CD57, a marker of terminally differentiated human NK cells (11), was detected in a few NK cells of hu-HSC NOG–IL-2 Tg mice, whereas CD57$^+$ cells constituted a considerable fraction of the normal PB-NK population (Fig. 3C). CD127, a marker of cytokine-producing NK cells, also was detected in a small subset of NK cells in hu-HSC NOG–IL-2 Tg mice (Fig. 3C).

KIR molecules are essential for NK cells to detect malignancy of target cells and to avoid responses to self-tissues. The KIR family consists of 15 genes and two pseudogenes, including both inhibitory and activating receptors. The KIR allele has two haplotypes (A and B), and the structure of the gene contents of KIR members can produce no less than 500 genotypes (The Allele Frequency Net Database, http://www.allelefrequencies.net/). KIR typing revealed that hu-HSC in NOG–IL-2 Tg mice contained a diverse repertoire of NK cells comparable to that foundin normal human NK cells from PB (Fig. 4A, Table II). In NK cells in hu-HSC NOG–IL-2 Tg mice with HSC from different ethnic origins, we detected differences in both haplotype and genotype, reflecting the origins of HSCs (Table II). FACS staining showed that NK cells in hu-HSC NOG–IL-2 Tg mice contained subpopulations expressing CD158b (KIR2DL2/3), CD158a/h (KIR2DL1/S1), or CD158e1 (KIR3DL, NKB1) (Fig. 4B).

Human NK cells develop in the BM through four distinct stages (12) (Fig. 5A). According to the classification, we assessed maturation of NK cells in hu-HSC NOG and NOG–IL-2 Tg mice. Flow cytometric analyses detected all stages of NK precursors in the BM of hu-HSC NOG–IL-2 Tg mice (Fig. 5B). In contrast, a small number of stage II NK precursors was detected in hu-HSC NOG, whereas there were few stage I, III, or IV cells (Fig. 5B, 5C). Mature NK cells accumulated in the spleen of hu-HSC NOG–IL-2 Tg mice, whereas few were identified in hu-HSC non-Tg NOG (Fig. 5D, 5E).

Mature human NK cells consist of two main subpopulations with differing functions: CD56^{bright}CD16$^-$ cells act as cytokine producers (13–15), and CD56^{dim}CD16$^+$ cells act as cytotoxic effector cells (16, 17). We confirmed the presence of these two subpopulations in the spleen and PB of hu-HSC NOG–IL-2 Tg mice (Figs. 5D, 6A). In hu-HSC non-Tg NOG, there were a few

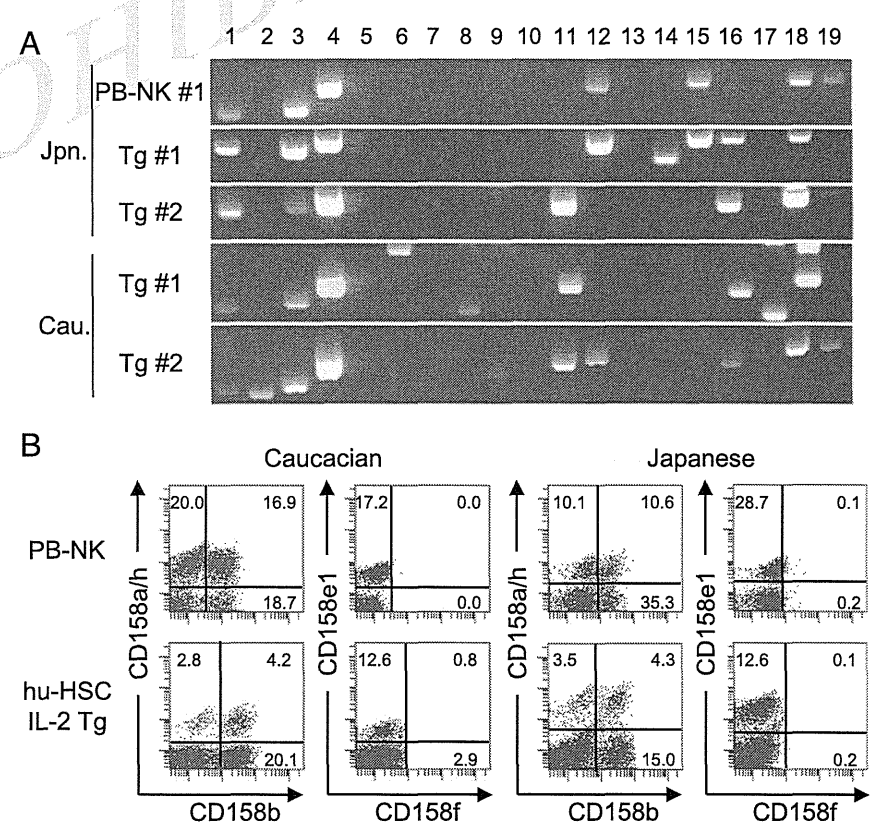

FIGURE 4. Expression of KIR molecules in human NK cells in hu-HSC NOG–IL-2 Tg mice. (**A**) Kirotyping by RT-PCR. Total RNA was isolated from three independent hu-HSC NOG–IL-2 Tg mice with HSCs from Japanese and white and normal human PB-NK cells. After cDNA synthesis, the KIR species in each sample were typed. The results are shown in Table I. (**B**) Representative FACS plots of human KIR are shown. Splenocytes of hu-HSC NOG–IL-2 Tg mice 6 wk after HSC transplantation and normal human CD56$^+$ PB-NK cells, which were negatively selected by MACS, were stained with Abs and analyzed. Representative data from three independent experiments are shown.

Table II. KIR repertoire of human NK cells of PB-NK and hu-HSC NOG–IL-2 Tg mice

			1	2	3	4	5	6	7	8	9	10	11	12	13	14	15	16	17	18	19
			2DL							2DS						3DL			3DS	2DP	3DP
	Lane		1	2	3	4	5all	5A	5B	1	2	3	4del	4ins	5	1	2	3	1	1	1
Japanese	PB-NK	1	+	|	+	+	|	|	|	|	|	|	|	+	|	+	|	+	|	+	|
		2	+	|	+	+	|	|	|	|	|	|	+	|	+	+	+	|	+	+	+
		3	+	|	+	+	|	|	|	|	|	|	+	|	+	|	+	|	+	+	|
	hu-HSC IL-2 Tg	1	+	|	+	+	|	|	|	|	|	|	+	|	+	|	+	|	+	+	+/−
		2	+	|	+	+	|	|	|	|	|	+	+	|	+	|	+	|	+	+	|
		3	+	|	+	+	|	|	|	|	|	|	+	|	+	|	+	|	+	+	|
		4	+	|	+	+	|	|	|	|	|	|	+	|	+	|	+	|	+	+	|
White	hu-HSC IL-2 Tg	1	+	|	+	+	|	+	|	+	|	|	+	|	|	|	+	|	+	+	|
		2	+	+	+	+	|	|	|	|	+	+	+	|	|	+	|	+	+	+	+
		3	+	+	+	+	|	|	|	|	|	|	|	|	|	+	|	+	+	+	+

Q:32

CD56^{bright}CD16^{-} cells (Fig. 6A). At 3 wk post-HSC transplantation, 40% of NK cells were CD56^{bright}CD16^{-} cells and 10% were CD56^{dim}CD16^{+} cells in the PB. At 6 wk, the proportion of the former decreased to 20% of NK cells, whereas the latter population showed a marginal increase (Fig. 6B, *upper panel*). In the spleen, ~60 and ~10% of NK cells were CD56^{bright}CD16^{-} and CD56^{dim}CD16^{+} cells, respectively, at 3 wk (Fig. 6B, *lower panel*). At 6 wk, the frequency of CD56^{bright}CD16^{-} cells decreased to 40%, whereas the size of the CD56^{dim}CD16^{+} cell population did not change significantly. These results indicated that the various subsets of human NK cells were uniquely distributed among the organs and that the changes in composition were tissue dependent.

In addition to CD56^{bright}CD16^{-} and CD56^{dim}CD16^{+} cells, hu-HSC NOG–IL-2 Tg mice showed characteristic accumulation of CD56^{bright}CD16^{+} cells (Fig. 6A). This fraction represented 40–50% of these cells in the PB and was relatively Q:18 constant over the experimental period (Fig. 6B). In the spleen, in contrast, this population made up ~30% of human NK cells at 3 wk post-HSC transfer and increased to 50% at 6 wk (Fig. 6B). We confirmed the expression of KIRs in this fraction, which suggested that they were mature, rather than immature, NK cells (data not shown).

The most prominent feature of NK cells is their cytolytic activity. We initially examined the expression of CD107a, a marker of degranulation, and found that it was present on the surface of NK cells in hu-HSC NOG–IL-2 Tg mice, suggesting that they were actively secreting cytolytic granules (Fig. 7A). We then F7 quantified granzyme A and perforin mRNA in the NK cells of hu-HSC NOG–IL-2 Tg mice by qPCR. The levels of granzyme A mRNA in NK cells of hu-HSC NOG–IL-2 Tg mice were ~2-fold those of PB-NK cells, whereas the perforin mRNA level in the former was half that of the latter (Fig. 7B), although the differences did not reach statistical significance. Intracellular staining showed that NK cells from hu-HSC NOG–IL-2 Tg produced abundant granzyme A, comparable to levels in human PB-NK cells, consistent with the qPCR results (Fig. 7C). Intracellular perforin staining showed that NK cells from hu-HSC NOG–IL-2 Tg produced a considerable level of perforin, although it was lower than that of human PB-NK cells (Fig. 7C). Nevertheless, hu-HSC NOG–IL-2 Tg mouse plasma contained a considerable amount of perforin (Fig. 7D). Taken together, these observations suggest active production of perforin by NK cells in hu-HSC NOG–IL-2 Tg mice.

To evaluate the cytotoxicity of NK cells in hu-HSC NOG–IL-2 Tg mice, we used the K562 cell line, which is susceptible to lysis by human NK cells, as a target in vitro. NK cells from hu-HSC NOG–IL-2 Tg mice showed significant cytotoxicity against K562 cells but not against HeLaS3 cells, as in the case of normal PB-NK cells (Fig. 8A). However, the cell killing activity was F8 lower than that of normal PB-NK cells, which was consistent with the low level of perforin expression. Because exogenous IL-2 or IL-12 could induce phosphorylation of the respective STAT molecules in NK cells from hu-HSC NOG–IL-2 Tg mice (Fig. 8B, data not shown), we examined whether the cytotoxicity could be recovered by cytokine stimulation. As expected, the addition of these cytokines markedly augmented the cytotoxicity (Fig. 8C). We also examined the IFN-γ–producing ability of NK cells from hu-HSC NOG–IL-2 Tg mice; stimulation with PMA and ionomycin or with IL-12 induced significant IFN-γ production (Fig. 8D).

Finally, we examined whether NK cells in hu-HSC NOG–IL-2 Tg mice had the ability to control the growth of tumor cells in vivo. We inoculated K562 s.c. into hu-HSC NOG–IL-2 Tg

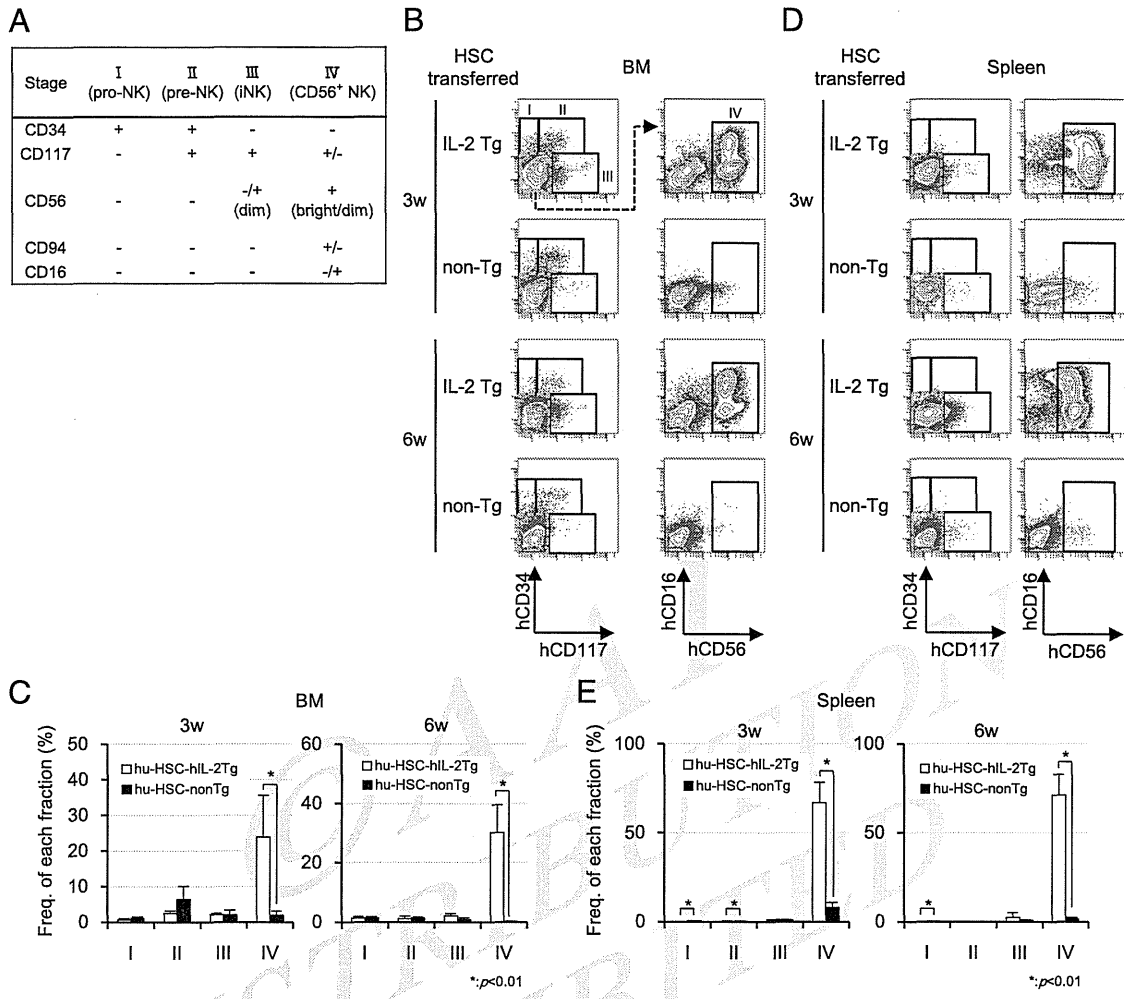

FIGURE 5. Progress of human NK cell differentiation in hu-HSC NOG–IL-2 Tg mice. (**A**) Human NK cell differentiation to show NK cell precursors. (**B** and **D**) Developmental course of human NK cells in hu-HSC NOG–IL-2 Tg mice. Based on the criteria shown in (A), BM (**B**) and spleen cells (**D**) of hu-HSC NOG–IL-2 Tg and non-Tg NOG mice were stained with the indicated Abs and analyzed for NK cell precursors. Each stage of NK precursor is denoted in the rectangular gates, as shown in (B). Mice were used at 3 wk (n =6 for Tg; n = 4 for non-Tg) and 6 wk (n = 5 for both groups) after HSC transplantation. Frequencies of subpopulations of NK precursors in BM (**C**) and spleen (**E**) are shown as percentages of total human CD45$^+$ cells. Student t test was used for identifying significant differences. Q:28

mice at 4 wk post-HSC transplantation. The tumor growth was almost completely inhibited (Fig. 9A). The number of human NK cells increased continuously over the experimental period (Supplemental Fig. 1). We also tested hu-HSC non-Tg NOG mice at 4 or 20 wk post HSC-transplantation as control. The former had a few human cells, whereas the latter had human cell numbers as high as those in the hu-HSC NOG–IL-2 Tg mice, but most of them were human T and B lymphocytes (Supplemental Fig. 1). In these control mice, K562 grew, regardless of the presence of human lymphocytes (Fig. 9A).

We next examined ADCC activity of human NK cells in hu-HSC NOG–IL-2 Tg in vivo. For this experiment, we used a combination of Hodgkin's lymphoma cell line, L428, and defucosylated chimeric anti-human CCR4 mAb (Poteligeo), because previous studies demonstrated that the normal human NK cells from PBMCs suppressed the growth of L428 in NOG mice in the presence of anti-CCR4 mAb (18). L428 expressed high levels of CCR4 (Supplemental Fig. 2). We inoculated 5 × 10^6 L428 in NOG–IL-2 Tg mice, with or without HSC transplantation, and the anti-CCR4 therapeutic Ab was administered twice each week for 4 wk. Tumor growth in hu-HSC NOG–IL-2 Tg mice was suppressed significantly compared with that in NOG–IL-2 Tg mice, suggesting that human NK cells killed the tumor in a manner similar to the that in K562 leukemia cells (Fig. 9B, Table III). T3 Although anti-CCR4 mAb treatment in NOG–IL-2 Tg mice had Q:19 no effect on tumor growth, anti-CCR4 Ab treatment further en- Q:20 hanced tumor suppression in hu-HSC NOG–IL-2 Tg mice (Fig. 9B, Table III). These results suggested that human NK cells developed in NOG–IL-2 Tg mice mediated ADCC and suppressed tumor growth.

Discussion

We demonstrated that NOG–IL-2 Tg mice showed long-lasting development of phenotypically mature human NK cells from HSCs in vivo. We also demonstrated that the human NK cells that developed in NOG–IL-2 Tg mice exhibited cytotoxicity against tumor cells in vitro, as well as in vivo through NK cell receptor–mediated mechanisms and by ADCC. Because of the abundant development of human NK cells, this mouse strain is suitable for in vivo analysis of human NK cells.

Previous in vitro studies demonstrated that IL-2 increased the number of human NK cells (19, 20) and selectively enhanced NK differentiation from HSCs (21). The >10-fold increase in the absolute number of human NK cells in NOG–IL-2 Tg mice

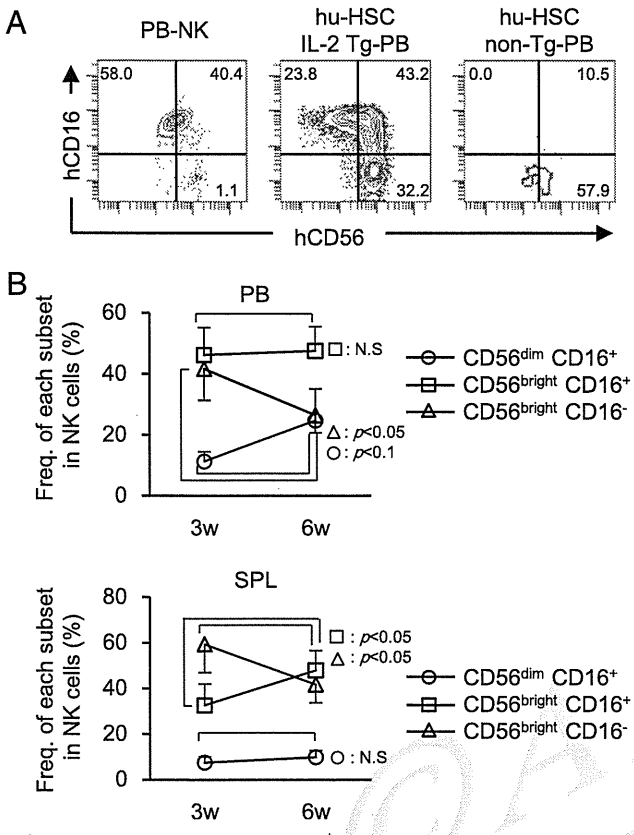

FIGURE 6. Presence of both $CD16^+$ and $CD16^-$ subfractions in human $CD56^+$ NK cells of hu-HSC NOG–IL-2 Tg mice. (**A**) FACS plots of human PB-NK and human NK cells in hu-HSC NOG–IL-2 Tg mice. Human NK cells in PB of hu-HSC NOG–IL-2 Tg mice 6 wk after HSC transplantation and normal human $CD56^+$ PB-NK cells were stained with anti-CD56 and CD16 Abs and analyzed by FACS. (**B**) Frequencies of $CD56^{dim}CD16^+$, $CD56^{bright}CD16^+$, and $CD56^{bright}CD16^-$ cells in the spleen (SPL) and PB were analyzed by FACS at 3 and 6 wk after HSC transplantation ($n = 6$ and 5, respectively). Each symbol represents the mean ± SD. The p values were calculated using the Student two-tailed t test.

compared with conventional NOG mice was consistent with the results of in vitro studies. The in vivo induction of human NK cells provided further information regarding the differentiation and distribution of human NK cells, which could not be obtained by in vitro experiments. The analysis of BM demonstrated clear differences in the development of NK cells between hu-HSC NOG–IL-2 Tg mice and hu-HSC NOG mice. The BM in the former had significant numbers of $CD34^-CD117^+$ immature NK (iNK) cells (stage III) and $CD56^+$ NK cells (stage IV), whereas the latter had few of these cells. Because pre-NK (stage II) cells were present in the BM in hu-HSC NOG mice, IL-2 may stimulate the differentiation of pre-NK (stage II) to iNK (stage III) cells. Alternatively, IL-2 may be indispensable for the survival of iNK cells. The massive increase in the number of stage IV NK cells in hu-HSC NOG–IL-2 Tg mice suggests that IL-2 also acted on this population. It is possible that IL-2 induced the proliferation and/or accumulation of stage IV cells. The cellular and molecular mechanisms involved in the enhanced NK differentiation remain to be clarified.

In the periphery, the phenotype of human NK cells in hu-HSC NOG–IL-2 Tg mice seemed to be different from that of normal PB-NK cells. Normal PB-NK cells consist of $CD56^{bright}CD16^-$ and $CD56^{dim}CD16^+$ cells as two major subpopulations, whereas in hu-HSC NOG–IL-2 Tg mice, in addition to these two subsets, $CD56^{bright}CD16^+$ cells constituted a considerable proportion of the NK population. Although this is an unusual NK population, clinical studies have provided some insights. For example, NK cells that initially appear after HSC transplantation are $CD56^{bright}$ NK cells (22–24). Although these cells have been considered to represent immature $CD56^{bright}$ NK cells, a recent report suggested that they were more likely to be mature NK cells activated by high levels of cytokines in patients (25). It is also important to note that $CD56^{bright}CD16^+$ NK cells accumulated in patients treated with a low dose of IL-2 (26). Intriguingly, these NK cells in IL-2–treated patients were similar to $CD56^{bright}CD16^+$ NK cells in hu-HSC NOG–IL-2 Tg mice, not only in their phenotype but also in terms of cytotoxicity (i.e., ex vivo NK cells in both cases did not show high cytotoxicity without in vitro cytokine stimulation). Thus, $CD56^{bright}CD16^+$ NK cells in hu-HSC NOG–IL-2 Tg mice have similarities to these cytokine-activated NK cells. This was further supported by the increases in CD107a, HLA-DR, and CD69 expression. The decrease in NKp80 was reported recently to be associated with NK cell activation (27). In addition, expression of various KIRs in human NK cells in hu-HSC NOG–IL-2 Tg mice represented strong evidence that they are mature NK cells. Nevertheless, the presence of a small number of $CD57^+$ NK cells in hu-HSC NOG–IL-2 Tg mice indicated that IL-2 does not always induce terminal differentiation of human NK cells.

The origin of the $CD56^{bright}CD16^+$ NK cells and their relationship to $CD56^{bright}CD16^-$ and $CD56^{dim}CD16^+$ cells in hu-HSC NOG–IL-2 Tg mice have not been clarified. The inversely proportional changes in $CD56^{bright}CD16^+$ NK cells and $CD56^{bright}CD16^-$ cells in the spleen over the experimental period suggested that the latter is the cellular origin of the former. However, in the PB, such a transition seems to be limited, because the frequency of $CD56^{bright}CD16^+$ NK cells was relatively constant. Rather, the kinetic changes in the frequencies of $CD56^{bright}CD16^-$ and $CD56^{dim}CD16^+$ populations in the PB indicate direct differentiation from the former to the latter, as suggested previously (5). The distinction in the composition of human NK subsets between the PB and the spleen suggests that the spleen is not always simply a reservoir of circulating NK cells and that the distribution is regulated differently, depending on the tissue, by unknown mechanisms. Human studies demonstrated that the frequencies of $CD56^{bright}CD16^-$ and $CD56^{dim}CD16^+$ cells differed between PB and secondary lymphoid organs; $CD56^{dim}CD16^+$ cells were predominant in PB, whereas $CD56^{bright}CD16^-$ constituted a considerable fraction in secondary lymphoid organs (28). Although the mechanisms responsible for the differences in localization have not been elucidated, it is possible that the distribution of human NK cells in hu-HSC NOG–IL-2 Tg mice was similarly regulated; therefore, this mouse strain may be useful in studies of these mechanisms.

A study using BALB/C-$RAG2^{-/-}$-IL-$2R\gamma c^{-/-}$ (BRG) mice transplanted with human HSCs demonstrated that administration of IL-15/IL-15Rα complexes induced linear differentiation of human NK cells from $CD56^{high}CD16^-$ to $CD56^{dim}CD16^+$ stages (5), suggesting that NK cell differentiation was recapitulated in the mouse environment. In this setting, $CD56^{bright}CD16^+$ NK cells were not detected. There are several possible explanations for the differences between the BRG experiment and our observations. First, NOG–IL-2 Tg mice provide a continuous IL-2 signal, whereas the effect of the IL-15 signal in the BRG system is transient. If $CD56^{bright}CD16^+$ NK cells represent the status of chronically activated NK cells, the short-term presence of IL-15 does not seem to be sufficient for the development of this population. Second, the amount and intensity of cytokine signals

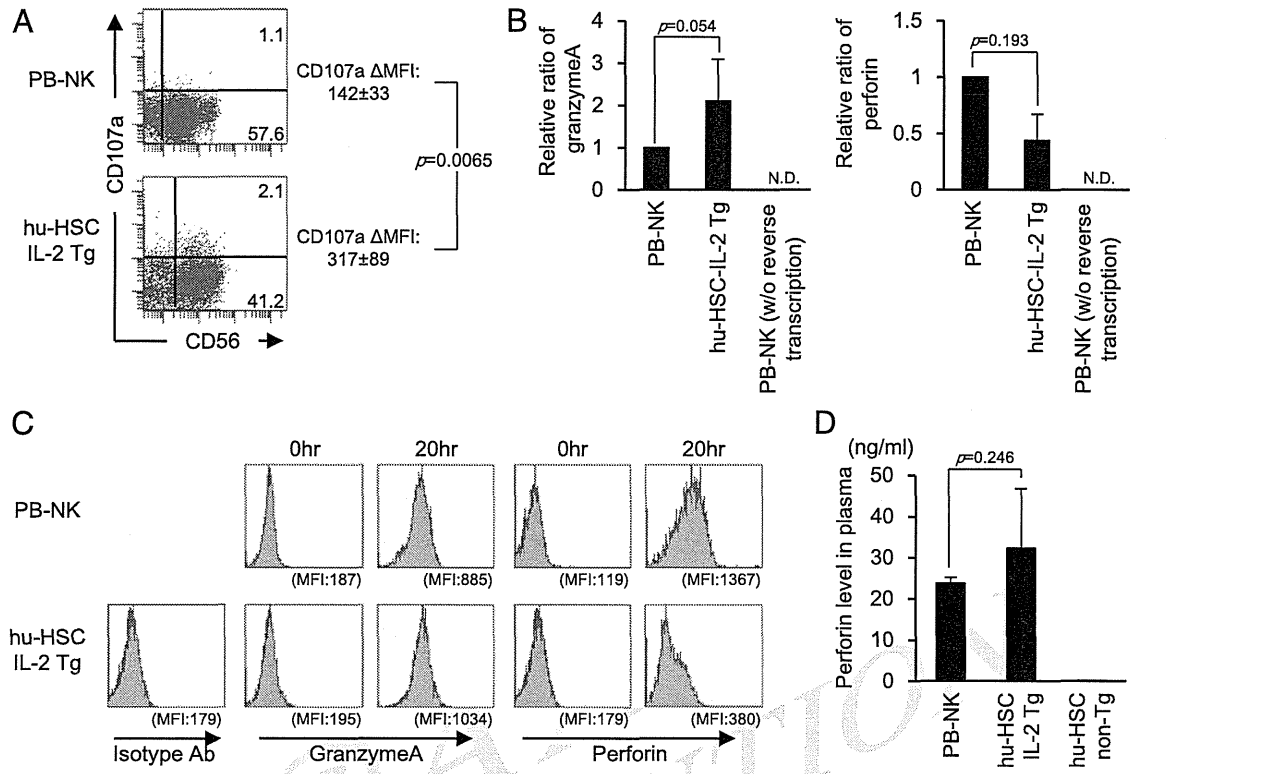

FIGURE 7. Production of granzyme and perforin in human NK cells of NOG–IL-2 Tg mice. (**A**) Expression of CD107a on human NK cells in hu-HSC NOG–IL-2 Tg mice. A single-cell suspension of splenocytes from hu-HSC NOG–IL-2 Tg mice was stained with anti-CD56 and anti-CD107a Abs and analyzed by FACS. Representative results from five independent mice are shown. (**B**) qPCR of granzyme A and perforin in NK cells. NK cells were isolated from hu-HSC NOG–IL-2 Tg mice and human PB-NK cells, and the expression levels of granzyme A and perforin mRNA were determined by qPCR. The mRNA amounts in NK cells from hu-HSC NOG–IL-2 Tg mice were normalized to those in PB-NK cells. Total RNA from PB-NK cells without reverse transcription was used as a negative control. The means (± SD) of four independent donors and five independent mice are shown. (**C**) Intracellular staining of granzyme A and perforin in human NK cells. Human NK cells purified from the spleens of hu-HSC NOG–IL-2 Tg mice and hPBMCs were cultured in the presence of brefeldin A for 20 h. Cells were stained with anti–granzyme A or anti-perforin mAb after fixation and permeabilization. The mean fluorescence intensity (MFI) of each graph is shown in parentheses. Representative data from three independent experiments are shown. (**D**) Quantification of perforin in plasma. The levels of perforin protein in plasma from normal healthy donors or hu-HSC NOG–IL-2 Tg mice were measured by ELISA. The mean (± SD) of three independent mice from each group are shown. The Student *t* test was used to identify significant differences.

would influence differentiation. The IL-2 concentration in the plasma of NOG–IL-2 Tg mice was ~1–3 ng/ml, which is sufficient to activate human NK cells. In contrast, levels of the exogenous IL-15/IL-15Rα complex decrease gradually to amounts that are insufficient to induce $CD56^{bright}CD16^{+}$ NK cells. Third, there are qualitative differences between IL-2 and IL-15: IL-15 is indispensable for NK development, and IL-2 is not (29–31), although these two cytokines have common signaling receptors. These three possibilities are not mutually exclusive and may act together to produce the differences between NOG–IL-2 Tg and BRG systems.

The in vitro analyses of the cytotoxicity of human NK cells in hu-HSC NOG–IL-2 Tg mice were confounding. The low level of perforin detected by qPCR and intracellular staining seems to be inconsistent with the presence of the protein in plasma. One possibility is that human NK cells aberrantly secrete perforin in response to IL-2, resulting in the accumulation in plasma. The presence of CD107a on the cellular surface of human NK cells in hu-HSC NOG–IL-2 Tg would support this idea (Table I). Another strange feature of human NK cells in hu-HSC NOG–IL-2 Tg mice is that they required additional cytokine stimulation to induce the in vitro cytotoxicity. Because the preculture without cytokine did not restore the cytotoxicity, the refractory state is not simply due to transient starvation of perforin. Chronic exposure to IL-2 might render human NK cells totally dependent on cytokine stimulation. It is important to clarify what kinds of molecular mechanisms (e.g., signal transductions, epigenetic changes) are involved in the alternation of NK cell functions.

The in vivo rejection of K562 and ADCC activity against L428 cells suggested that human NK cells exposed to continuous IL-2 stimulation had the potency to delineate and kill malignant cells using their receptor systems, including NCR, the NKG2 family, KIRs, and CD16. These results raise two important questions. The first concerns "licensing" or "education" of NK cells. The second question is how human NK cells in hu-HSC NOG–IL-2 Tg mice are kept in check in the absence of human HLA. Recent studies suggested that NK cells require interactions between their inhibitory receptors and the corresponding ligands (e.g., KIRs and class I HLA) (32, 33). Because there have been no reports regarding mouse orthologs of HLA-C, which are major ligands for multiple inhibitory KIRs, the "NK cell licensing" hypothesis suggests the hyporesponsiveness of human NK cells in hu-HSC NOG–IL-2 Tg mice. The in vivo killing activity is contrary to the expectation. One possible explanation is that NK cells acquire functional competency through interactions between KIRs and class I HLA in HSC-derived donor hematopoietic cells. Whether NK cells receive sufficient signals for maturation under these conditions remains to be addressed. It will be of interest to produce a novel NOG strain expressing the HLA-C gene or NOG–HLA-C/IL-2

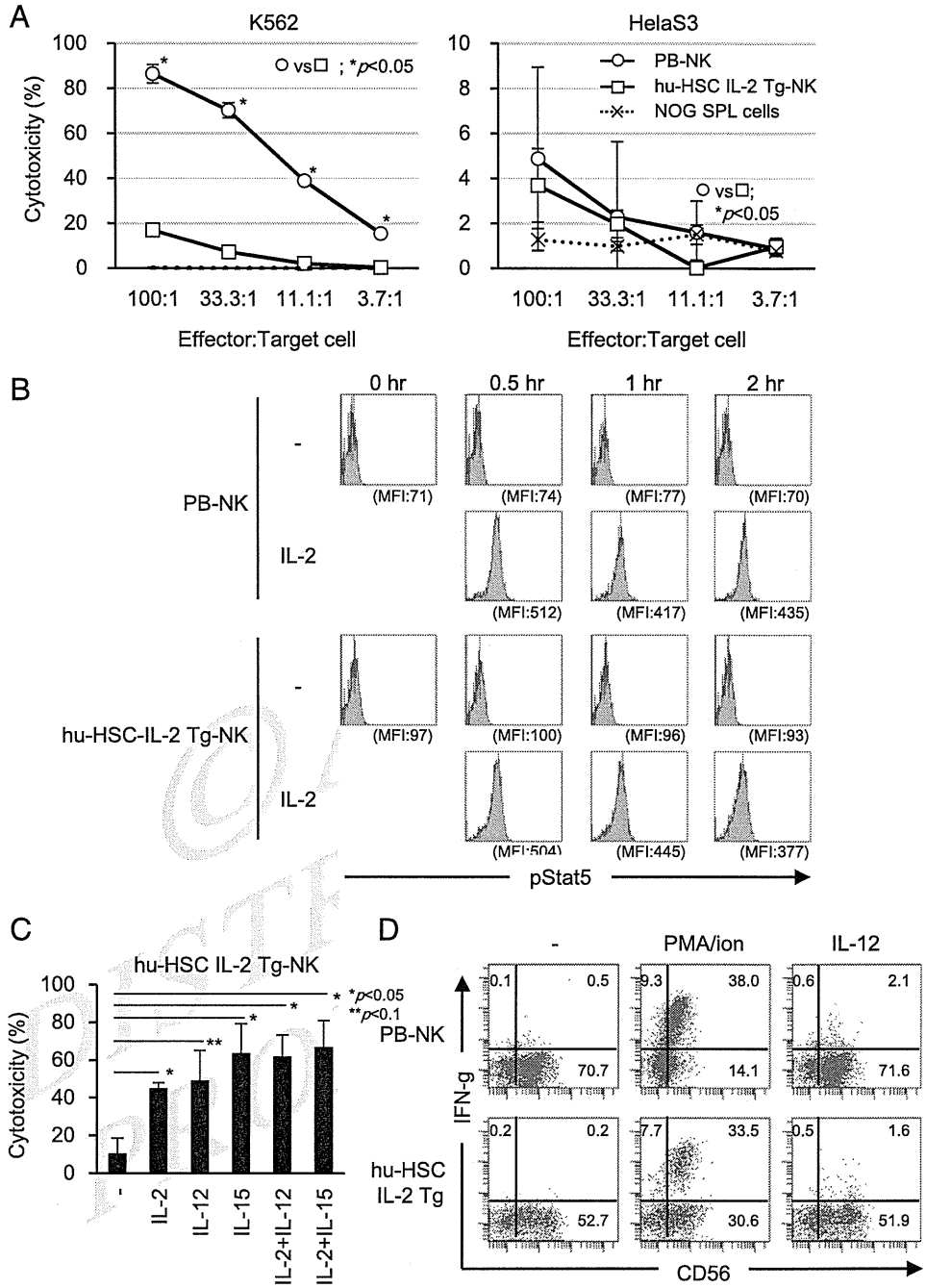

FIGURE 8. Function of human NK cells in hu-HSC NOG–IL-2 Tg mice. (**A**) Natural cytotoxicity of human NK cells was examined in vitro. Normal human PB-NK cells (○) or splenic NK cells pooled from three hu-HSC NOG–IL-2 Tg mice (□), 6 wk post-HSC transplantation, were cultured with ^{51}Cr-labeled human tumor cell lines (K562, *left panel*; HeLaS3, *right panel*) as targets for 4 h. Target cell lysis was measured by the ^{51}Cr level in culture supernatants. The averages ± SD of triplicate cultures are plotted for each point. Representative data from two independent experiments are shown. (**B**) Phosphorylation of STAT5 in NK cells in hu-HSC NOG–IL-2 Tg mice by IL-2 stimulation. PB-NK or splenic NK cells from hu-HSC NOG–IL-2 Tg mice were cultured in the presence or absence of rIL-2 for the indicated periods. After stimulation, cells were fixed and permeabilized as described in *Materials and Methods*. After staining with anti–phospho-STAT5 Ab, cells were subjected to flow cytometric analysis. Representative results from $n = 2$ are shown. (**C**) Augmentation of cytotoxicity in NK cells of hu-HSC NOG–IL-2 Tg mice by cytokine stimulation. Human NK cells purified from the spleens of hu-HSC NOG–IL-2 Tg mice were stimulated with human IL-2, IL-12, and IL-15 for 48 h. These cytokine-activated human NK cells were recovered and cultured with K562 at an E:T ratio of 10:1 for 4 h in vitro. The release of lactate dehydrogenase in the culture supernatants was measured using a CytoTox96 Non-Radioactive Cytotoxicity Assay kit. The average of duplicate cultures for each indicated cytokine stimulation is plotted. (**D**) Production of IFN-γ by human NK cells in hu-HSC NOG–IL-2 Tg mice. Purified human NK cells were cultured with human IL-12 or PMA/ionomycin for 20 h in the presence of brefeldin A. After fixation and permeabilization, cells were stained with anti-CD56 and anti–IFN-γ Abs. Representative data from two independent experiments are shown. The Student *t* test was used to identify significant differences.

double-transgenic mice, in which "license" signals are provided by mouse stromal cells, and compare their NK characters with those in NOG–IL-2 Tg mice.

With regard to the tolerance of human NK cells in hu-HSC NOG–IL-2 Tg mice, mouse experiments showed that NK cells have the ability to change their responsiveness upon encountering

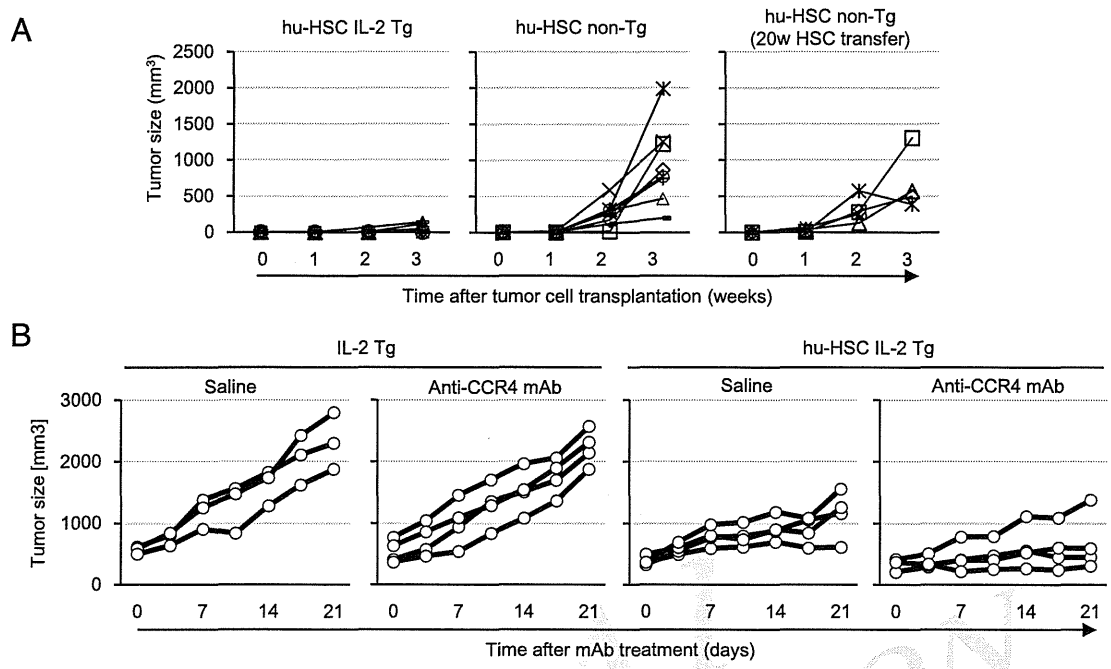

FIGURE 9. In vivo tumor suppression by human NK cells in hu-HSC NOG–IL-2 Tg mice. (**A**) Tumor growth in HSC-transplanted mice. hu-HSC NOG–IL-2 Tg mice and non-Tg NOG mice, at 4 wk post-HSC transplantation, or non-Tg NOG mice, at 20–24 wk post-HSC transfer, were inoculated s.c. with 2.5×10^5 K562. The arrows indicate the elapsed times after tumor inoculation. The size of the K562 tumor was measured each week after inoculation. Cumulative data are shown, which were obtained from three independent experiments using a total of 10 independent hu-HSC NOG–IL-2 Tg mice and 8 non-Tg NOG mice at 4 wk post-HSC transplantation and 5 non-Tg NOG mice at 20 wk post-HSC transfer. (**B**) hu-HSC NOG–IL-2 Tg mice and non-transplanted NOG–IL-2 Tg mice at 3 wk post-HSC transplantation were inoculated s.c. with 5×10^6 L428. At 3 wk post-L428 transplantation, 100 μg of anti-CCR4 mAb mogamulizumab was injected i.p. into the tumor-bearing mice twice each week for 3 wk. The size of the L428 tumor was measured every 3–4 d during mogamulizumab treatment. The arrow indicates the elapsed times after tumor inoculation. Cumulative data are shown, which were obtained from one representative experiment using a total of eight independent hu-HSC NOG–IL-2 Tg mice and seven nontransplanted NOG–IL-2 Tg mice. Statistical analyses are summarized in Table III.

alterations in MHC environments (34, 35). When mature NK cells from normal mice were transferred into syngeneic β2m-deficient ($\beta2m^{-/-}$) mice, the production of IFN-γ or killing of $\beta2m^{-/-}$ was reduced significantly (34, 35). Although the mechanisms responsible for the plasticity of NK cells have not been elucidated, it is possible that the activity of human NK cells in hu-HSC NOG–IL-2 Tg mice is similarly regulated in the absence of class I MHC signals in the recipient mouse environment. This raises the question of how hu-HSC NOG–IL-2 Tg mice control tumor cells. It is likely that human NK cells in hu-HSC NOG–IL-2 Tg mice use activating NK receptors, NCRs, NKG2D, and CD16, which do not use classical class I HLA, as ligands. The former two receptors recognize signals from "stressed-self," which is often expressed by various tumor cells, and so the human NK cells in hu-HSC NOG–IL-2 Tg mice would receive sufficient stimulation to eliminate them. The stimulatory role of CD16 was clearly demonstrated by the experiment using the anti-CCR4 mAb. In addition, IL-2 in this environment augments the responsiveness, as shown in the in vitro study.

The in vivo ADCC activity suggested that hu-HSC NOG–IL-2 Tg mice have an important practical application in that this strain provides an ideal experimental system for the development of therapeutic mAbs. As mAbs are essential drugs in molecular targeted therapy, our hu-HSC NOG–IL-2 Tg mice will be a useful mouse model in which the ability of candidate Abs to induce ADCC can be objectively evaluated in vivo. The predominance of human NK cells excludes any possible interference by other cell types, and the long-term production of NK cells enables prolonged experiments, both of which are important advantages over other animal models.

In conclusion, we generated a novel mouse strain, NOG–IL-2 Tg, which can induce predominant human NK cells from HSCs. This new mouse strain will facilitate in vivo analysis of human NK cells and promote the development of better strategies for the treatment of various diseases. Q:22

Q:33 Table III. Summary of statistical tests for in vivo ADCC using anti-CCR4 mAb and hu-HSC NOG–IL-2 Tg mice

	p Values						
	Day						
	0	4	7	11	14	18	21
IL-2 Tg saline vs. IL-2 Tg anti-CCR4 mAb	0.413	0.434	0.248	0.489	0.364	0.175	0.385
hu-HSC IL-2 Tg saline vs. hu-HSC IL-2 Tg anti-CCR4 mAb	0.121	0.007	0.031	0.035	0.105	0.110	0.094
IL-2 Tg saline vs. hu-HSC IL-2 Tg saline	0.008	0.042	0.043	0.075	0.015	0.011	0.012
IL-2 Tg anti-CCR4 mAb vs. hu-HSC IL-2 Tg anti-CCR4 mAb	0.040	0.030	0.027	0.006	0.006	0.001	0.001

Acknowledgments

We thank Dr. Ishida for kindly providing L428. We thank Masashi Sasaki for technical assistance, Kayo Tomiyama and Yasuhiko Ando for animal production and care, and Dr. Masafumi Yamamoto for genotyping. We also thank Dr. James P. Di Santo (Institut Pasteur, Paris, France) for critical reading of the manuscript and helpful discussions.

Disclosures

The authors have no financial conflicts of interest.

References

1. Spits, H., and J. P. Di Santo. 2011. The expanding family of innate lymphoid cells: regulators and effectors of immunity and tissue remodeling. *Nat. Immunol.* 12: 21–27.
2. Timonen, T. 1997. Natural killer cells: endothelial interactions, migration, and target cell recognition. *J. Leukoc. Biol.* 62: 693–701.
3. Shiokawa, M., T. Takahashi, A. Murakami, S. Kita, M. Ito, K. Sugamura, and N. Ishii. 2010. In vivo assay of human NK-dependent ADCC using NOD/SCID/gammac(null) (NOG) mice. *Biochem. Biophys. Res. Commun.* 399: 733–737.
4. Hiramatsu, H., R. Nishikomori, T. Heike, M. Ito, K. Kobayashi, K. Katamura, and T. Nakahata. 2003. Complete reconstitution of human lymphocytes from cord blood CD34+ cells using the NOD/SCID/gammacnull mice model. *Blood* 102: 873–880.
5. Huntington, N. D., N. Legrand, N. L. Alves, B. Jaron, K. Weijer, A. Plet, E. Corcuff, E. Mortier, Y. Jacques, H. Spits, and J. P. Di Santo. 2009. IL-15 trans-presentation promotes human NK cell development and differentiation in vivo. *J. Exp. Med.* 206: 25–34.
6. Strowig, T., O. Chijioke, P. Carrega, F. Arrey, S. Meixlsperger, P. C. Rämer, G. Ferlazzo, and C. Münz. 2010. Human NK cells of mice with reconstituted human immune system components require preactivation to acquire functional competence. *Blood* 116: 4158–4167.
7. Chen, Q., M. Khoury, and J. Chen. 2009. Expression of human cytokines dramatically improves reconstitution of specific human-blood lineage cells in humanized mice. *Proc. Natl. Acad. Sci. USA* 106: 21783–21788.
8. Willinger, T., A. Rongvaux, T. Strowig, M. G. Manz, and R. A. Flavell. 2011. Improving human hemato-lymphoid-system mice by cytokine knock-in gene replacement. *Trends Immunol.* 32: 321–327.
9. Shultz, L. D., M. A. Brehm, J. V. Garcia-Martinez, and D. L. Greiner. 2012. Humanized mice for immune system investigation: progress, promise and challenges. *Nat. Rev. Immunol.* 12: 786–798.
10. Ito, R., T. Takahashi, I. Katano, and M. Ito. 2012. Current advances in humanized mouse models. *Cell. Mol. Immunol.* 9: 208–214.
11. Lopez-Vergès, S., J. M. Milush, S. Pandey, V. A. York, J. Arakawa-Hoyt, H. Pircher, P. J. Norris, D. F. Nixon, and L. L. Lanier. 2010. CD57 defines a functionally distinct population of mature NK cells in the human CD56dimCD16+ NK-cell subset. *Blood* 116: 3865–3874.
12. Freud, A. G., A. Yokohama, B. Becknell, M. T. Lee, H. C. Mao, A. K. Ferketich, and M. A. Caligiuri. 2006. Evidence for discrete stages of human natural killer cell differentiation in vivo. *J. Exp. Med.* 203: 1033–1043.
13. Caligiuri, M. A., A. Zmuidzinas, T. J. Manley, H. Levine, K. A. Smith, and J. Ritz. 1990. Functional consequences of interleukin 2 receptor expression on resting human lymphocytes. Identification of a novel natural killer cell subset with high affinity receptors. *J. Exp. Med.* 171: 1509–1526.
14. Nagler, A., L. L. Lanier, S. Cwirla, and J. H. Phillips. 1989. Comparative studies of human FcRIII-positive and negative natural killer cells. *J. Immunol.* 143: 3183–3191.
15. Cooper, M. A., T. A. Fehniger, S. C. Turner, K. S. Chen, B. A. Ghaheri, T. Ghayur, W. E. Carson, and M. A. Caligiuri. 2001. Human natural killer cells: a unique innate immunoregulatory role for the CD56(bright) subset. *Blood* 97: 3146–3151.
16. Lanier, L. L., A. M. Le, J. H. Phillips, N. L. Warner, and G. F. Babcock. 1983. Subpopulations of human natural killer cells defined by expression of the Leu-7 (HNK-1) and Leu-11 (NK-15) antigens. *J. Immunol.* 131: 1789–1796.
17. Jacobs, R., G. Hintzen, A. Kemper, K. Beul, S. Kempf, G. Behrens, K. W. Sykora, and R. E. Schmidt. 2001. CD56bright cells differ in their KIR repertoire and cytotoxic features from CD56dim NK cells. *Eur. J. Immunol.* 31: 3121–3127.
18. Ito, A., T. Ishida, H. Yano, A. Inagaki, S. Suzuki, F. Sato, H. Takino, F. Mori, M. Ri, S. Kusumoto, et al. 2009. Defucosylated anti-CCR4 monoclonal antibody exercises potent ADCC-mediated antitumor effect in the novel tumor-bearing humanized NOD/Shi-scid, IL-2Rgamma(null) mouse model. *Cancer Immunol. Immunother.* 58: 1195–1206.
19. Trinchieri, G., M. Matsumoto-Kobayashi, S. C. Clark, J. Seehra, L. London, and B. Perussia. 1984. Response of resting human peripheral blood natural killer cells to interleukin 2. *J. Exp. Med.* 160: 1147–1169.
20. Lanier, L. L., D. W. Buck, L. Rhodes, A. Ding, E. Evans, C. Barney, and J. H. Phillips. 1988. Interleukin 2 activation of natural killer cells rapidly induces the expression and phosphorylation of the Leu-23 activation antigen. *J. Exp. Med.* 167: 1572–1585.
21. Miller, J. S., C. Verfaillie, and P. McGlave. 1992. The generation of human natural killer cells from CD34+/DR− primitive progenitors in long-term bone marrow culture. *Blood* 80: 2182–2187.
22. Jacobs, R., M. Stoll, G. Stratmann, R. Leo, H. Link, and R. E. Schmidt. 1992. CD16− CD56+ natural killer cells after bone marrow transplantation. *Blood* 79: 3239–3244.
23. Chklovskaia, E., P. Nowbakht, C. Nissen, A. Gratwohl, M. Bargetzi, and A. Wodnar-Filipowicz. 2004. Reconstitution of dendritic and natural killer-cell subsets after allogeneic stem cell transplantation: effects of endogenous flt3 ligand. *Blood* 103: 3860–3868.
24. Dulphy, N., P. Haas, M. Busson, S. Belhadj, R. Peffault de Latour, M. Robin, M. Carmagnat, P. Loiseau, R. Tamouza, C. Scieux, et al. 2008. An unusual CD56 (bright) CD16(low) NK cell subset dominates the early posttransplant period following HLA-matched hematopoietic stem cell transplantation. *J. Immunol.* 181: 2227–2237.
25. Vukicevic, M., Y. Chalandon, C. Helg, T. Matthes, C. Dantin, B. Huard, C. Chizzolini, J. Passweg, and E. Roosnek. 2010. CD56bright NK cells after hematopoietic stem cell transplantation are activated mature NK cells that expand in patients with low numbers of T cells. *Eur. J. Immunol.* 40: 3246–3254.
26. Caligiuri, M. A., C. Murray, M. J. Robertson, E. Wang, K. Cochran, C. Cameron, P. Schow, M. E. Ross, T. R. Klumpp, R. J. Soiffer, et al. 1993. Selective modulation of human natural killer cells in vivo after prolonged infusion of low dose recombinant interleukin 2. *J. Clin. Invest.* 91: 123–132.
27. Klimosch, S. N., Y. Bartel, S. Wiemann, and A. Steinle. 2013. Genetically coupled receptor-ligand pair NKp80-AICL enables autonomous control of human NK cell responses. *Blood* 122: 2380–2389.
28. Ferlazzo, G., D. Thomas, S. L. Lin, K. Goodman, B. Morandi, W. A. Muller, A. Moretta, and C. Münz. 2004. The abundant NK cells in human secondary lymphoid tissues require activation to express killer cell Ig-like receptors and become cytolytic. *J. Immunol.* 172: 1455–1462.
29. Kennedy, M. K., M. Glaccum, S. N. Brown, E. A. Butz, J. L. Viney, M. Embers, N. Matsuki, K. Charrier, L. Sedger, C. R. Willis, et al. 2000. Reversible defects in natural killer and memory CD8 T cell lineages in interleukin 15-deficient mice. *J. Exp. Med.* 191: 771–780.
30. Lodolce, J. P., D. L. Boone, S. Chai, R. E. Swain, T. Dassopoulos, S. Trettin, and A. Ma. 1998. IL-15 receptor maintains lymphoid homeostasis by supporting lymphocyte homing and proliferation. *Immunity* 9: 669–676.
31. Suzuki, H., G. S. Duncan, H. Takimoto, and T. W. Mak. 1997. Abnormal development of intestinal intraepithelial lymphocytes and peripheral natural killer cells in mice lacking the IL-2 receptor beta chain. *J. Exp. Med.* 185: 499–505.
32. Kim, S., J. Poursine-Laurent, S. M. Truscott, L. Lybarger, Y. J. Song, L. Yang, A. R. French, J. B. Sunwoo, S. Lemieux, T. H. Hansen, and W. M. Yokoyama. 2005. Licensing of natural killer cells by host major histocompatibility complex class I molecules. *Nature* 436: 709–713.
33. Kim, S., J. B. Sunwoo, L. Yang, T. Choi, Y. J. Song, A. R. French, A. Vlahiotis, J. F. Piccirillo, M. Cella, M. Colonna, et al. 2008. HLA alleles determine differences in human natural killer cell responsiveness and potency. *Proc. Natl. Acad. Sci. USA* 105: 3053–3058.
34. Joncker, N. T., N. Shifrin, F. Delebecque, and D. H. Raulet. 2010. Mature natural killer cells reset their responsiveness when exposed to an altered MHC environment. *J. Exp. Med.* 207: 2065–2072.
35. Elliott, J. M., J. A. Wahle, and W. M. Yokoyama. 2010. MHC class I-deficient natural killer cells acquire a licensed phenotype after transfer into an MHC class I-sufficient environment. *J. Exp. Med.* 207: 2073–2079.

AUTHOR QUERIES

AUTHOR PLEASE ANSWER ALL QUERIES 1

1—Please verify that the title, footnotes, author names, and affiliations are correct as set.

2—Please indicate the correct surname (family name) of each author for indexing purposes.

3—Please verify that the mailing address and e-mail address for correspondence are correct as set.

4—If your proof includes supplementary material, please confirm that all supplementary material is cited in the text.

5—If your proof includes links to Web sites, please verify that the links are valid and will direct readers to the correct Web page.

6—Please check article carefully throughout to verify that edits have preserved your intent.

7—Please confirm hu-HSC is correctly defined in the abstract and as added to the abbreviations footnote. Should this say "cord blood–derived human hematopoietic stem cells (hu-HSCs)" instead? Please amend as needed and reconcile with the abbreviations footnote and first appearance in text.

8—Please confirm edits to sentence "Taken together, these data suggest..." retain your intent. Please amend as needed.

9—Any alternations between capitalization and/or italics in genetic nomenclature have been retained per the original manuscript. Please confirm that all genetic nomenclature has been formatted properly throughout.

10—Please confirm the definition of "NOG–IL-2 Tg" is correct as edited. Please note the definitions in the Abstract, abbreviations footnote, and text must all match per style. If amending, please be sure to reconcile at all locations. Thank you.

11—Changed "RPMI" to "RPMI 1640" here ("The spleen, liver, lung, kidney, and heart...") at first appearance and throughout the text (8 instances total). Please amend or confirm as needed.

12—Please clarify sentence beginning "HSC-transferred mice were euthanized...." ("euthanized" versus "under anesthesia"). Please amend as needed.

13—"APC" was spelled out as "allophycocyanin" at all three appearance in the *Flow Cytometry* section. Per journal guidelines, APC is the standard abbreviation for "Ag-presenting cell" and may not be used as an abbreviation for a different term. Please amend or confirm.

14—

15—Please confirm "hu-HSC" has been correctly defined at first appearance in text. Please note the Abstract, Abbreviations, and first appearance in text must match per style. Please amend at all locations as needed.

AUTHOR QUERIES

AUTHOR PLEASE ANSWER ALL QUERIES 2

16—Please clarify sentence beginning "Most of the human CD45...". Would it be correct to say "Most of the human $CD45^+$ $CD56^-$ cells were comprised of $CD19^+$ B cells in the spleen and $CD33^+$ human myeloid cells in the liver and lung"? Please modify for intent.

17—Please confirm edits to sentence beginning "KIR typing revealed that hu-HSC NOG–IL-2..." retain your intent. Please amend as needed.

18—Please clarify "this fraction" in sentence beginning "This fraction represented 40–50% of these cells."

19—Please confirm edits to sentence beginning "Tumor growth in hu-HSC ..." retain your intent. Please amend as needed.

20—Please confirm edits to sentence beginning "Although anti-CCR4 mAb treatment in NOG–IL-2 Tg mice..." retain your intent. Please amend as needed.

21—Please clarify word choice "alternation of" in sentence beginning "It is important to clarify what kinds..."? Should it be "...involved in alternating NK cell functions" or "involved in the various NK cell functions"? Other? Please amend.

22—Please confirm that all potential conflicts of interest have been disclosed.

23—Please confirm location is correct as added for Institut Pasteur in the *Acknowledgments*.

24—Please confirm edits to legend for Fig. 1A retain your intent. Please amend as needed.

25—If your proof includes figures, please check the figures in your proof carefully. If any changes are needed, please provide a revised figure file.

26—Please provide the significance of or value for the single (*) and double (**) asterisks in Figure 1B and 1D.

27—Please provide the significance of or value for the single (*) asterisks in Figure 2.

28—Please provide the significance of or value for the single (*) asterisks in Figure 5C and 5E.

29—Please provide expansion for "N.S" in Figure 6.

30—Please provide expansion for "N.D." in Figure 7.

31—To what does "n = 2" refer in the legend for Fig. 8B?

32—Please provide explaination for "+" and "–" in a footnote for Table II.

AUTHOR QUERIES

AUTHOR PLEASE ANSWER ALL QUERIES 3

33—Please confirm heading "*p* Values" is correctly placed. In the original Table III, the heading was over column one, but the *p* values seem to be listed under the Days in columns two through eight. Please confirm.